

Research Article

Effect of Acid Activation-Hydrophilic-Modified Sepiolite on Comprehensive Properties of Oil-Well Cement

Yihang Zhang ¹, Miao He ¹, Mingbiao Xu ^{1,2} and Peng Xu¹

¹Petroleum Engineering College, Yangtze University, Wuhan 430100, China

²Hubei Cooperative Innovation Center of Unconventional Oil and Gas, Yangtze University, Wuhan 430100, China

Correspondence should be addressed to Miao He; hemiao@yangtzeu.edu.cn

Received 20 August 2019; Revised 28 October 2019; Accepted 18 November 2019; Published 11 December 2019

Academic Editor: Franck Rabilloud

Copyright © 2019 Yihang Zhang et al. This is an open access article distributed under the Creative Commons Attribution License, which permits unrestricted use, distribution, and reproduction in any medium, provided the original work is properly cited.

In this paper, sepiolite was treated by acid activation, coupling agent treatment, and sulfonation modification. The purpose of this study was to explore the changes in the fluidity and mechanical properties of sepiolite cement slurry before and after modification. Therefore, the comprehensive properties of unmodified sepiolite fiber (HPS) and acid activation-coupling agent treatment-sulfonated sepiolite fiber (S-O-H-HPS) in oil-well cement slurry were evaluated. FT-IR and microscopic mechanism of cement paste fracture surface before and after sepiolite modification were analyzed. The results showed that HPS can effectively improve the toughness of cement paste, but when the content of HPS was more than 1%, the fluidity of cement paste deteriorated sharply and the compressive strength decreased gradually. The addition of S-O-H-HPS can significantly improve the fluidity and stability of HPS slurry. Without affecting the compressive strength, it can effectively improve the flexural strength and impact strength and reduce the elastic modulus of cement paste. The mechanism analysis showed that S-O-H-HPS can not only form network structure in cement paste but also improve the toughness of cement paste by forming a bridge. This also explains why the strength of S-O-H-HPS cement paste does not decrease significantly with the increase of S-O-H-HPS.

1. Introduction

Cementing operation is very important in drilling engineering. The main purpose of cementing is to seal the oil, gas, and water layers in the wellbore, protect the casing of oil and gas wells, prolong the life of oil and gas wells, and increase the production of oil and gas wells [1–4]. However, in the process of cement slurry flow, it is inevitable to produce small bubbles, resulting in a decrease of cement strength. At the same time, when the cement solidifies, it will also be impacted and vibrated by the drill pipe and well-stimulation measures (perforation and fracturing) during the construction process, resulting in the failure of cement sealing [5, 6]. The main failure modes of cement sheath are transverse stresses failure, longitudinal stress failure, and microannulus (Figure 1).

According to the principle of super-hybrid composite [7], improving the plasticity of cement sheath and enhancing the deformation ability of cement sheath can effectively deal

with these defects [8]. The dynamic mechanical properties of cement paste can be effectively changed by adding fillers of appropriate types and characteristics in the cement slurry. It can not only reduce the elastic modulus of cement sheath and prevent the appearance of microcracks and microannulus but also improve the flexural and shear strengths of cement sheath. The most common toughening admixture is the fiber material [9]. The dynamic mechanical properties of the cement sheath are affected and improved by adding fiber structural material into cement composition, and the stress field at the crack tip is shielded to improve the fracture toughness of the cement slurry system.

Pizzol et al. [10] maximized the degradation of ligno-cellulose by accelerating carbonization in the hydration process of carbonized fiber cement. Mechanical property tests showed that the maximum load and toughness increased by about 25% and 80%, respectively. But it also needs a lot of dispersants. Li et al. [11] investigated the effect of methylcellulose and carboxymethyl cellulose on carbon

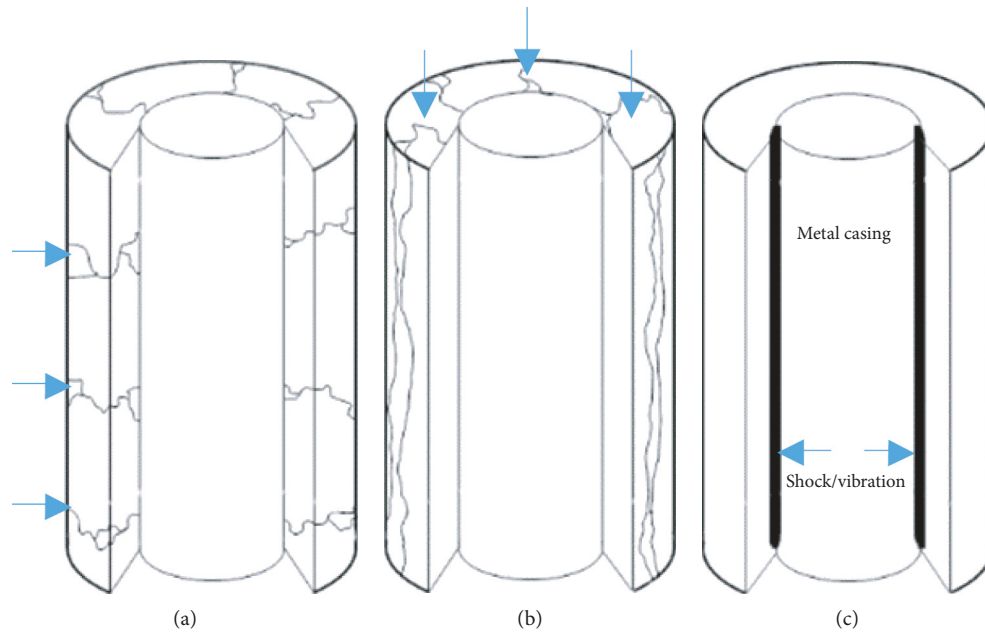


FIGURE 1: Several failure forms of cement rings: (a) transverse stresses failure; (b) longitudinal stress failure; (c) microannulus.

fibers. It was found that a 0.2 wt.% CMC solution could disperse carbon fibers effectively. The compressive strength, flexural strength, and splitting tensile strength of cement paste samples were increased by 8.6%, 31.5%, and 52.4%, respectively, with 0.3 wt.% carbon fiber addition. The elastic modulus of cement paste samples was reduced by 49.5% compared with pure cement samples. However, the fluidity of cement slurry becomes worse when the amount of carbon fiber is more than 3%, and its fluidity is only 17 cm. Cao et al. [12] studied the effect of CaCO_3 whisker on the mechanical properties of cement mortar. It was found that when the content of CaCO_3 whisker was in the range of 1.5–2.0%, its flexural strength and compressive strength increased by 27.59% and 12.60%, respectively. This is because CaCO_3 can not only improve the compactness of the cement matrix but also enhance the early hydration of cement [13–15]. However, when the amount of calcium carbonate whisker is more than 2%, its fluidity will decrease, and its initial consistency value is higher than $30B_C$, which is not conducive to cementing operation.

At present, there are mainly the following kinds of theories in explaining and analyzing the mechanism of fiber crack resistance and toughening.

1.1. Fiber Spacing Theory. The lack of toughness of cement paste begins with the original defects (pore, crack, etc.) existing in the interior, and the proper size and quantity of fibers can fill this part of the original hole [16], thus effectively reducing internal cracks, preventing crack propagation, and playing a certain role in crack prevention.

1.2. Composite Material Theory. There is a linear relationship between the strength and elastic modulus of cement paste and matrix and fibers. The strength of composites increases

linearly with the increase of fiber content and strength [17]. Of course, the problem of fiber-toughening the cement stone is more obvious: too little dosage, and the toughening effect is not good; the increase of fiber dosage will lead to poor mixing fluidity and cost increase. Secondly, toxic fibers (for example, asbestos fibers) need to be taken into account in order to meet the current requirements of environmental protection operations in oilfields. Therefore, in this paper, sepiolite with long fiber structure, high temperature and salt resistance, good corrosion resistance, environmental protection, and pollution-free property is selected as the basic toughening fiber material.

Sepiolite is a 2:1 layered chain clay with the characteristics of chain and layered fibrous transition structure [18, 19]. Its relative density is 2.0–2.6, its suspension ($\omega=10\%$) pH value is about 9, sepiolite is a gray-white flowing powder [20–22], and its general formula is $(\text{Si}_{12})(\text{Mg}_8)\text{O}_{30}(\text{OH})_4(\text{OH}_2)_4 \cdot 8\text{H}_2\text{O}$. The projection of the sepiolite unit cell on the (001) plane is shown in Figure 2.

Due to the high impurity content of natural sepiolite minerals, narrow pore channels, and low specific surface area, the effect of natural sepiolite as a cement composite material is greatly affected [23–26]. In this paper, sepiolite fibers (acid activation) were purified and modified by coupling agent modification and sulfonation treatment. The performance difference and improvement degree of blank cement stone, and S-O-H-HPS cement stone samples were compared. The structure, morphology, and dispersion degree of products at different stages were characterized and analyzed by FT-IR and SEM.

2. Experiment

2.1. Materials. G-grade oil-well cement, the raw material, was purchased from Sichuan Jiahua Enterprise (Group) Co.,

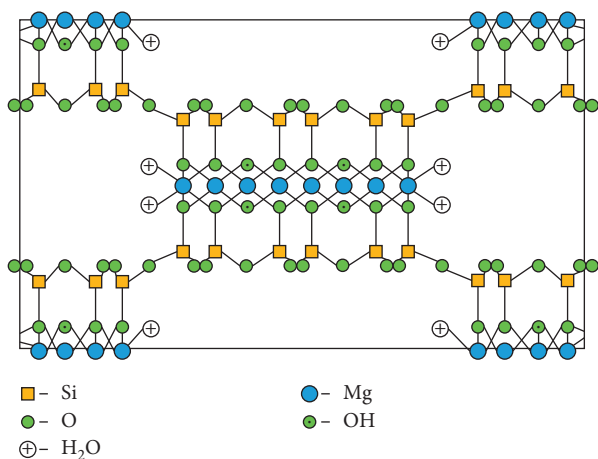
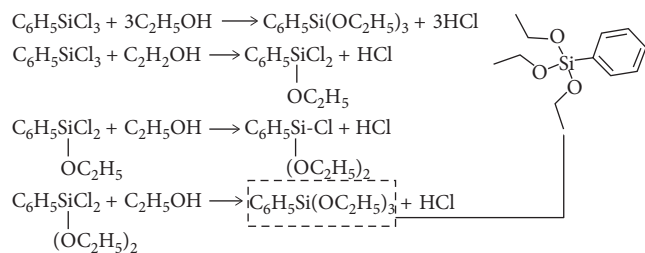


FIGURE 2: Projection of sepiolite unit cell on the (001) plane.

Ltd. Sepiolite fibers (fiber shape with processing growth of 0.1–0.8 cm; aspect ratio of 1 : 4–1:15; specific gravity: 2.8–3.2; tensile strength: 874.5–1257.3 MPa) its basic composition are shown in Table 1. Dispersant, retarder, enhancers, filtrate reducer, and defoamer were kindly provided by Jingzhou Jiahua Technology Co., Ltd. Phenyltrichlorosilane, and anhydrous methanol (analytical purity) were provided by Shandong Yukang Chemical Co., Ltd. Hydrochloric acid, sulfuric acid, isopropanol, and ethanol of analytical purity were provided by Nanjing Golden Chemical Co., Ltd. The composition of the experimental formula is shown in Table 2.

2.2. Synthetic Methods

2.2.1. Synthesis of Coupling Agents. In this experiment, the coupling agent was prepared by the liquid-phase method (the reaction formula presented as follows). Quantitative phenyltrichlorosilane was weighed in three flasks, and anhydrous ethanol was dripped at room temperature. After 10 hours, it was heated to 100°C in a vacuum environment. Cooling water was released by condensation. The content of chlorine and the pH value of the crude product were determined and the system was cooled to room temperature [27, 28]. Subsequently, the product is then obtained by fractionation.



2.2.2. Sepiolite Acid Activation Treatment. 8–10 wt.% sepiolite fiber was weighed and placed in a beaker. 90 wt.% hydrochloric acid solution (1.6 mol/L) was added and stirred for 10 minutes. Subsequently, it was placed at room

temperature for 5 minutes. The foam residues were removed from the solution surface, and it was transferred to a three-necked flask and stirred for 6 hours at 70°C. Then, the product was washed with absolute ethanol and deionized water until neutral. The activated sepiolite was dried and ground.

2.2.3. Hydrophilic Surface Modification of Activated Sepiolite.

Samples of 30 wt.% activated sepiolite were dispersed and mixed with 500 mL isopropanol at room temperature for 3 hours. The coupling agent was added to three flasks and stirred continuously for a whole night. Then, the flasks were cooled to room temperature. After washing with absolute ethanol, the samples were washed with deionized water to neutral. After drying and grinding in the oven, the coupling agent-modified sepiolite (O-H-HPS) fibers were obtained.

2.2.4. Sulfonated-Modified Sepiolite.

Sulfonated-modified sepiolite (S-O-H-HPS) was prepared by adding O-H-HPS to a certain amount of concentrated sulfuric acid, stirring continuously for a whole night, and washing with deionized water until it was completely neutral.

2.3. Cement Slurry Preparation.

The preparation of cement slurry was carried out according to the relevant regulations of GB 10238–2005 “Oil Well Cement.” The slurry water and other additives were weighed by using a mixing mug cup and then placed on the base of the constant-speed mixer to stir at the rotational speed of 4000 + 200 r/min. At the same time, the cement ash and the modified external filler are evenly added within 15 s. When the mixing was complete, the mixing speed was 10,000 (±500 r/min) and the mixing time was 35 (±1 s) for a total of 50 s. When the rotation stopped, the cup was removed and the mixing process was complete.

2.4. Conventional Performance Testing of Cement Slurry

2.4.1. Rheological Testing. According to the oil industry standard SY/T5546-92 “Test method for application performance of oil well cement” and API specification “Standard and experimental specification for oil well cement materials,” shear stress at different rotational speeds was measured, and its averaged value was tested four times, and rheological parameters were calculated through the following formulas:

$$\begin{aligned}
 n &= 2.096 \lg \left(\frac{\phi_{300}}{\phi_{100}} \right), \\
 k &= 0.511 \left(\frac{\phi_{300}}{511^n} \right),
 \end{aligned} \tag{1}$$

where n represents the fluidity index, dimensionless, and k represents the consistency coefficient, Pa·s ^{n} .

2.4.2. Testing of Thickening Time. The thickening time of cement slurry was measured by using a pressure thickener, and the sealing of the assembled slurry cup was maintained during the testing process. This comparative experiment

TABLE 1: Sepiolite component.

Component	SiO ₂	TiO ₂	Al ₂ O ₃	Fe ₂ O ₃	FeO	MnO	CaO	MgO	Na ₂ O
Content (%)	55.3	0.001	0.46	0.41	0.09	0.002	0.06	24.52	0.03

TABLE 2: Slurry components of different modified sepiolite contents.

No.	Cement	Water	Dispersant	Enhancer	Retarder	Defoamer	Expanding agent	Filtrate reducer
Cement	800	370	4	16	2	3	8	18
Cement + 0.5% HPS	800	370	4	16	2	3	8	18
Cement + 1.0% HPS	800	370	5	16	2	3	8	18
Cement + 1.5% HPS	800	370	6	16	2	4	8	18
Cement + 2.0% HPS	800	370	8	16	2	5	8	18
Cement + 2.5% HPS	800	370	—	16	2	6	8	18
Cement + 3.0% HPS	800	370	—	16	2	6	8	18
Cement + 5.0% HPS	800	370	—	16	2	7	8	18
Cement + 7.0% HPS	800	370	—	16	2	8	8	18
Cement + 9.0% HPS	800	370	—	16	2	8	8	18
Cement + 0.5% H-HPS/S-O-H-HPS	800	370	4	16	2	3	8	18
Cement + 1.0% H-HPS/S-O-H-HPS	800	370	4	16	2	3	8	18
Cement + 1.5% H-HPS/S-O-H-HPS	800	370	4	16	2	3	8	18
Cement + 2.0% H-HPS/S-O-H-HPS	800	370	4	16	2	3	8	18
Cement + 2.5% H-HPS/S-O-H-HPS	800	370	4	16	2	3	8	18
Cement + 3.0% H-HPS/S-O-H-HPS	800	370	4	16	2	3	8	18
Cement + 5.0% H-HPS/S-O-H-HPS	800	370	4	16	2	3	8	18
Cement + 7.0% H-HPS/S-O-H-HPS	800	370	4	16	2	3	8	18
Cement + 9.0% H-HPS/S-O-H-HPS	800	370	4	16	2	3	8	18

Units: g.

recorded the time when the consistency reached 100 Bc under the condition of 80 °d × 45 MPa, which was used as the final thickening time of cement slurry.

2.4.3. API Water Loss Measurement. The cement slurry with good mixing quality was maintained at 80 °C for 20 minutes by using an ambient temperature densifier, and then, it was taken out to mix evenly in the slurry cup. Then, the cement slurry was transferred to a high-temperature and high-pressure water-loss meter, and the water loss of the cement slurry at 80 °C × 6.9 MPa for 30 minutes was measured.

2.4.4. Free Liquid Test. The cement slurry treated by using curing strip at 80 °C under normal pressure was poured into a 250 mL measuring cylinder to obtain the premeasured volume V_s , and then, the volume V_f of free liquid (chromatographic water) was measured after 2 hours. Free liquid integral F was calculated according to the following formula:

$$F = \left(\frac{V_f}{V_s} \right) \times 100\%. \quad (2)$$

2.5. Mechanical Property Testing

2.5.1. Preparation of Test Samples. The prepared cement slurry is poured into the curing die for testing compressive strength, flexural strength, and impact strength and sealed by using a cover plate after being coated with sealing grease. Then, the mould with samples was put into the TG-7370D

pressurized maintenance kettle (Liaoning Bassett Petroleum Equipment Manufacturing Co., Ltd.) and maintained at 80 °L × 21 MPa (pressure and temperature control) for a certain time, and then, the mould was taken out for demoulding.

2.5.2. Performance Test. After cooling the demoulded sample to room temperature, the compressive strength and elastic modulus of cement paste were tested by using a TH-8100S universal testing machine (Suzhou Tuobo Machinery Equipment Co., Ltd.) and the flexural strength was tested by replacing the testing components and the impact strength of cement spline was tested by using a FURBS-FBS impact strength testing machine (Xiamen Forbes Testing Equipment Co., Ltd.). All the test samples were tested 4–8 times to get the average value and recorded.

2.6. Structural Analysis

2.6.1. Microscopic Morphology Observation of Cement Stone. The fragments of cement paste after compressive strength tests on a universal testing machine were collected. The surface of the fragments was smooth and pollution free. The micromorphology of the cement paste section was observed by using a HITACHI SU-8010 scanning electron microscope.

2.6.2. FT-IR Analysis. The instrument used in this experiment was the Bruker Tensor II spectrometer. The product was extracted by using acetone and then dried. The sulfonated-modified dried HPS sample (2.0 mg) and KBr

powder were ground uniformly and pressed. The scanning range was $4000\text{--}600\text{ cm}^{-1}$. The final absorption spectrum was obtained after repeated scanning.

3. Results and Discussion

3.1. Structural and Morphological Analyses. As shown in Figure 3, FT-IR measurements of acid-activated sepiolite fibers/sepiolite powder and composite-modified sepiolite fibers showed the strength of the characteristic peaks at 3446 cm^{-1} and 1643 cm^{-1} of the samples modified by using hydrophilic coupling agent A and by sulfonation decreased significantly. The 743 cm^{-1} exhibited the characteristic peaks of silicone phenyl, and the symmetric peak of $-\text{CH}_2$ in coupling agent A appeared newly at 2925 cm^{-1} . At the same time, the peak width increased around 1071 cm^{-1} , which was due to the overlap of the characteristic peak area of the sulfonic acid group with the silica characteristic peak in sepiolite structure.

3.2. Effect of Sulfonated Sepiolite on Conventional Properties of Cement Slurry. In the process of cementing operation, cementing slurry not only has good rheological properties to improve pumping efficiency but also needs better thickening controllable time, lower water loss and better slurry stability. The basic performance is the precondition for subsequent performance evaluation experiments. The evaluation experiments of cement slurry foundation performance under different dosages of HPS and S-O-H-HPS were carried out indoors. The results are shown in Table 3. It can be seen from the table that the incorporation of unmodified HPS has a great influence on the rheological properties of the cement slurry. With the increase of HPS dosage, the fluidity index n of cement slurry decreased dramatically and the consistency coefficient increased obviously. It was difficult to agitate the slurry when the dosage was increased to 3% or more; even if the dosage of the dispersant was increased, it was difficult to improve, which was consistent with the defect of conventional fibers when they were used as tougheners for cement. The fluidity index n of S-O-H-HPS admixture cement slurry decreased slowly with the increase in S-O-H-HPS (0%–9%). The decrease of n value was obviously smaller than that of HPS admixture cement slurry. At the same time, the consistency coefficient K was much lower than that of HPS, and the fluidity of slurry was better than that of HPS cement paste. This showed that the addition of S-O-H-HPS greatly reduced the difficulty of cement slurry preparation. At the same time, the increment interval was enlarged. The reason was that after acid activation, on the one hand, calcite impurities between the pores of sepiolite were removed and on the other hand, Mg^{2+} in sepiolite skeleton was removed and transformed into silicon oxide of the Si-OH group. With the increase of specific surface area, the internal channel increased significantly and the pore size increased [29–31].

At the same time, the stability of cement paste with HPS and S-O-H-HPS fibers was tested. The results are shown in

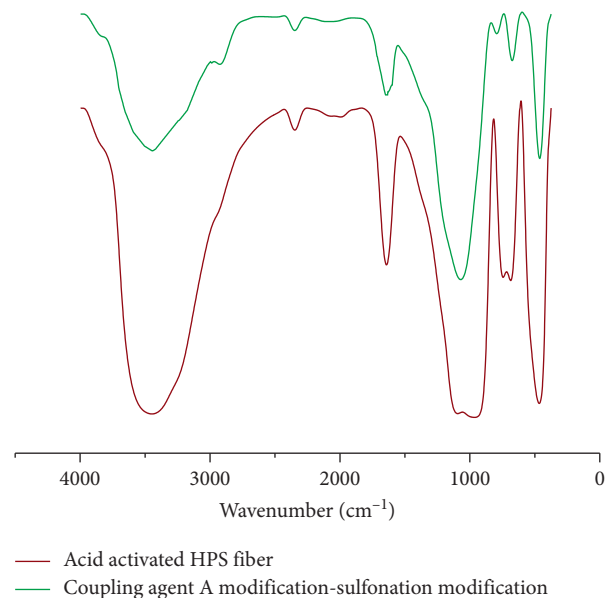


FIGURE 3: FT-IR spectra of acid-activated HPS fiber and coupling agent modification-sulfonation modification.

TABLE 3: Rheological properties of modified cement slurry.

Dosage (%)	HPS		S-O-H-HPS	
	n	K	n	K
0	0.84	0.36	0.84	0.36
1	0.71	0.86	0.8	0.39
3	0.55	1.54	0.71	0.53
5	0.32	1.86	0.63	0.84
7	0.2	2.35	0.5	0.95
9	—	—	0.41	1.24

Tables 4 and 5. It can be seen from the table that with the increase of HPS dosage, the fluidity of cement slurry decreased obviously, the slurry became thicker, and the density difference increased gradually, while for S-O-H HPS-admixed cement slurry, the fluidity and density difference were less affected by the dosage. This showed that the dispersion of HPS fibers had been greatly improved after modification.

Figure 4 shows that with the increase of HPS and S-O-H-HPS content, the filtration loss of cement slurry decreased continuously. Among them, the filtrate loss of cement slurry with S-O-H HPS was lower than that with HPS.

Figure 5 shows that the thickening time of cement paste will be more prolonged with the increase of HPS and S-O-H-HPS. Within the range of 0%–3% addition, the maximum thickening time was prolonged by about 70 minutes, and there was no significant difference in the thickening time among sepiolite types.

3.3. Effect of Sulfonated Sepiolite on Mechanical Properties of Cement Slurry. In order to determine the change of the comprehensive properties of sulfonated sepiolite to cement stone, the mechanical properties of cement slurry need to be

TABLE 4: Effect of HPS dosage on the stability of cement slurry.

HPS dosage (%)	Free fluid (mL)	Density difference ($\text{g}\cdot\text{cm}^{-1}$)
0	0	0.01
1	0	0.01
3	0	0.01
5	0	0.02
7	0	0.03
9	0	0.04

TABLE 5: Effect of S-O-H HPS dosage on the stability of cement slurry.

S-O-H-HPS dosage (%)	Free fluid (mL)	Density difference ($\text{g}\cdot\text{cm}^{-1}$)
0	0	0.01
1	0	0.01
3	0	0.02
5	0	0.01
7	0	0.01
9	0	0.01

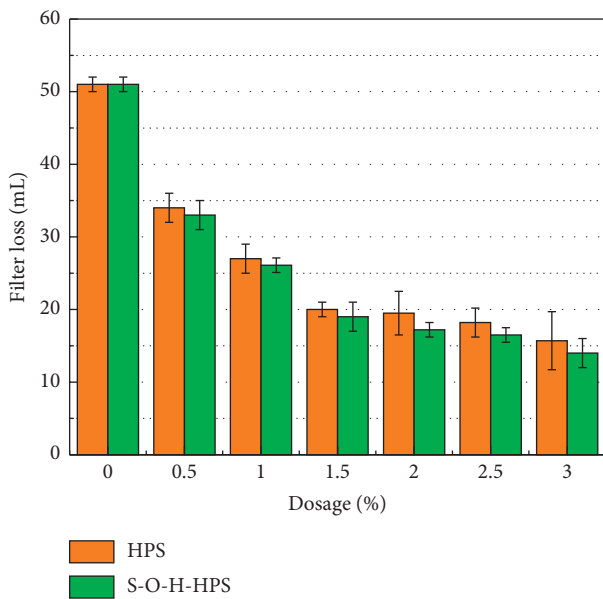


FIGURE 4: Variation of cement slurry filtration with HPS and S-O-H-HPS additions.

investigated. Based on this, the mechanical properties of cement paste with different HPS and S-O-H-HPS additions were evaluated and compared. The evaluation results are shown in Figures 6–9.

From Figures 6 and 7, it can be seen that with the increase of HPS content, the compressive strength of cement stone mixed with HPS decreased continuously, while the S-O-H-HPS-admixed cement paste samples after modification fluctuated smoothly and the compressive strength did not decrease significantly. From Figure 7, it can be seen that the modulus of elasticity of S-O-H-HPS

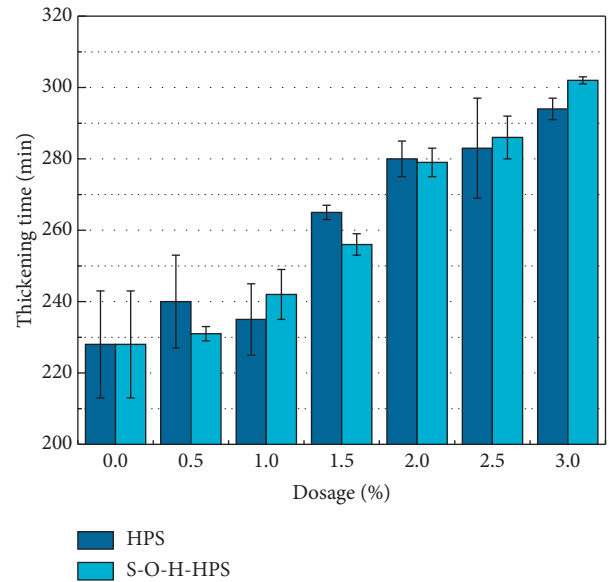


FIGURE 5: Variation of cement slurry thickening time with HPS, H-HPS, and S-O-H-HPS dosage.

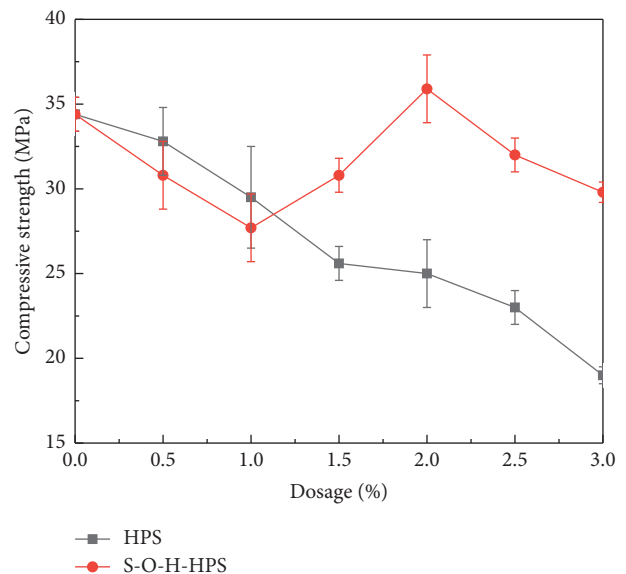


FIGURE 6: Effect of additives on compressive strength of cement paste.

admixture decreased more than that of unmodified HPS cement paste.

From Figure 8, it can be seen that with the increase of HPS and S-O-H-HPS, the impact strength of S-O-H-HPS and unmodified HPS increased obviously when the content was less than 1.5% and then increased steadily. Among them, the impact strength of S-O-H-HPS admixed cement stone increased mostly than that of a blank sample at 2.5%, reaching 16.1%.

From Figure 9, it can be seen that with the increase of HPS and S-O-H-HPS additions, the shear strength of HPS increased first and then decreased, with a maximum increase of 25.4%

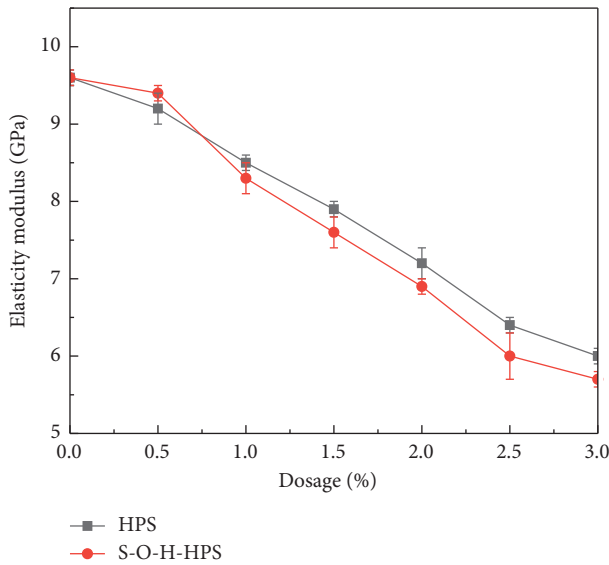


FIGURE 7: Effect of additives on elastic modulus of cement paste.

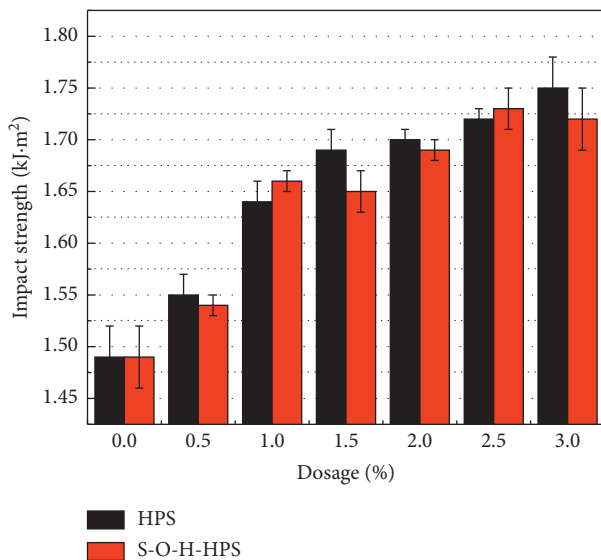


FIGURE 8: Effect of additive on impact strength of cement stone.

under 2%, while that of S-O-H-HPS increased first and then remained stable, with a maximum increase rate of 35%.

3.4. Effect of Curing Age on Mechanical Properties of Cement Slurry. In view of the above considerations, the comprehensive performance of cement stone can be improved obviously by choosing 2.0%–2.5% S-O-H-HPS additive. Therefore, by choosing the 2%–2.5% S-O-H-HPS sample with better comprehensive performance, the mechanical properties of blank cement samples at different curing ages (1, 7, 14 days) were compared. Figure 10 shows that when the S-O-H-HPS additive was 2% and the compressive strength at different curing ages was all equal. Compared with blank cement samples, the compressive strength growth rate of blank cement samples increased by 4.4%, 7.4%, and 7.6% at 1

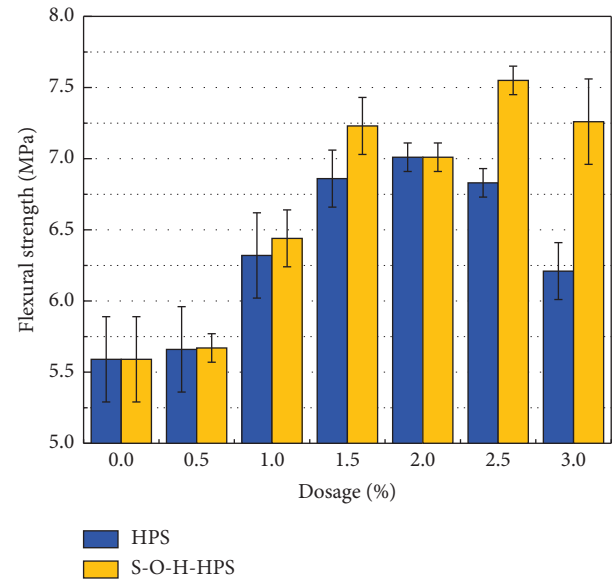


FIGURE 9: Effect of additives on shear strength of cement paste.

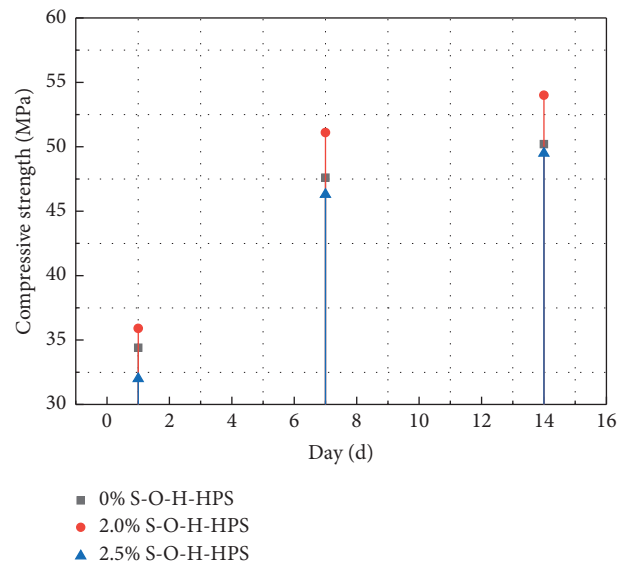


FIGURE 10: Effect of curing age on compressive strength of cement stone.

day, 7 day, and 14 day respectively, and the strength of 2.5% S-O-H-HPS cement samples at 1 day was lower than that of blank cement samples, but the strength values at 7 day and 14 day were shrinking continuously and the strength at 14 day was basically equal to that of blank cement samples.

Figure 11 shows that the shear strength of S-O-H-HPS at 2.0% and 2.5% was higher than that of blank cement stone. The shear strength of S-O-H-HPS at 2.0% was 25%, 19%, and 17.7% higher than that of blank cement stone at 1 d, 7 d, and 14 d, respectively. The shear strength of S-O-H-HPS at 2.5% is 35%, 27%, and 24.8% higher than that of blank cement stone at 1 d, 7 d, and 14 d, respectively.

Figure 12 shows that the impact strength of S-O-H-HPS at 2.0% and 2.5% was higher than that of blank cement stone. The impact strength of S-O-H-HPS at 2.0% was 13.4%,

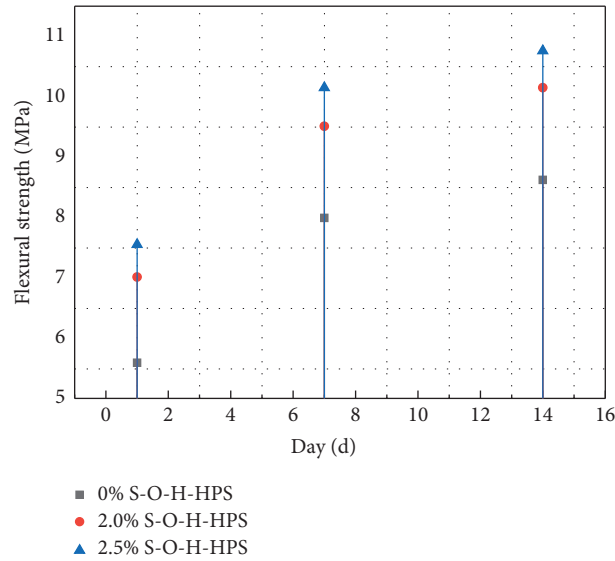


FIGURE 11: Effect of curing age on shear strength of cement stone.

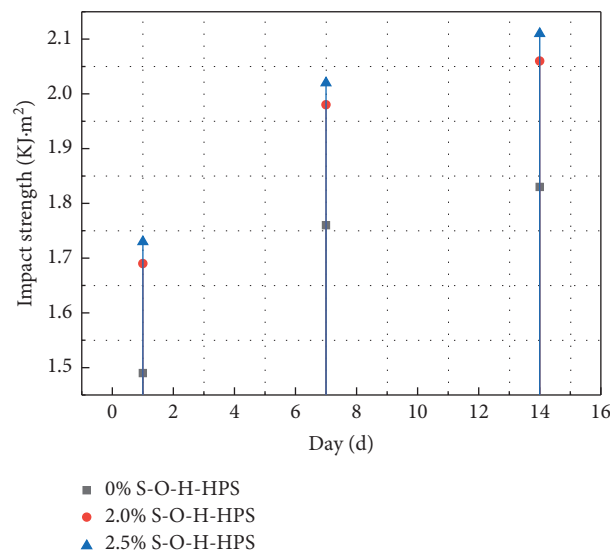


FIGURE 12: Effect of curing age on impact strength of cement paste.

12.5%, and 12.6% higher than that of blank cement stone at 1 d, 7 d, and 14 d, respectively. The impact strength of S-O-H-HPS at 2.5% was 16.1%, 14.8%, and 15.3% higher than that of blank cement stone at 1 d, 7 d, and 14 d, respectively.

3.5. Mechanism Analysis. Through the observation and analysis of the internal micromorphology of the cement paste with S-O-H-HPS (2.5%), we can see that the microstructure of the cement paste is shown in Figure 13. As can be seen from Figure 13, S-O-H-HPS acted on cement paste in two ways, one is bundle fiber structure (Figure 13(a)-A) and the other is reticular structure distribution (Figure 13(a)-B), in which reticular structure was mainly distributed in cement paste. Figures 13(b) and 13(c) are

enlarged treatment of these two structures, respectively. The reticular structure can work with hydration products without affecting the structure of hydration products. The results showed that the aggregates were uniform and dispersed, and there was no obvious agglomeration phenomenon, which made the compressive strength of cement paste to unchange greatly after S-O-H-HPS was admixed, and the mesh wire drawing structure effectively improved the bulk structure and mechanical properties of cement paste, while the bundle fiber structure in cement paste was relatively less distributed, which played an auxiliary toughening role. The “lacing wire-bridging (Figure 13(e))” mode was formed by interpenetrating the two ends of the fracture surface. It can improve the transverse ductility of cement paste and inhibit the development of microcracks of cement paste, thus

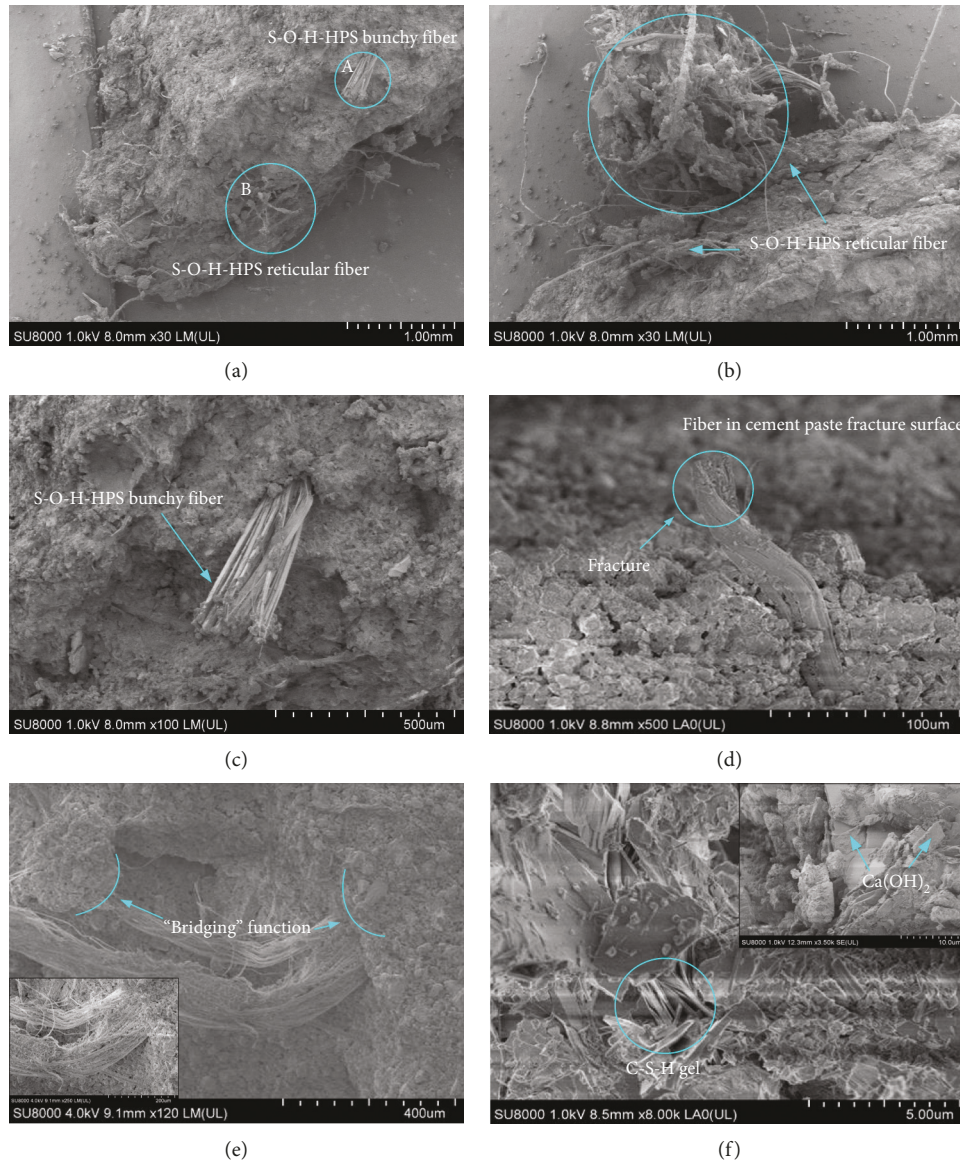


FIGURE 13: Micromechanism of sulfonated sepiolite fibers.

reducing the brittleness of cement paste and improving the toughness of the matrix.

4. Conclusion

On the basis of acid activation treatment of conventional sepiolite fibers, sepiolite was further modified by coupling agent modification and sulfonation treatment. By comparing the effect of unmodified sepiolite fiber (HPS) and acid activation-coupling agent treatment-sulfonated sepiolite fiber (S-O-H-HPS), the following conclusions were drawn:

- (i) Through the rheological test of cement slurry, it can be seen that when unmodified sepiolite fibers were used as admixtures of cement slurry, although the effect was obvious in improving the toughness of cement slurry, when the content of cement slurry was more than 1%, the fluidity of cement slurry was

extremely poor, which greatly increased the difficulty of slurry mixing and construction. At the same time, the strength attenuation was also obvious because of unmodified sepiolite fibers. The surface of treated sepiolite fibers was covered by dense zeolite water and adsorbed water, and the internal channels were blocked. The sepiolite fibers agglomerate and disperse unevenly in cement slurry making the stirring process more difficult.

- (ii) A series of evaluations of modified sepiolite fibers showed that the fluidity of cement paste was less affected by the addition of sepiolite fibers as admixtures of cement slurry and the dispersibility of sepiolite fibers was greatly improved. This was because some Mg^{2+} in sepiolite was replaced by H^+ and the junction of Mg^{2+} was lost after acid activation treatment. When water is constructed, Si-OH in the

framework increases, while coupling agent replaces part of zeolite water in sepiolite channel by condensation reaction with Si-OH and introduces benzene ring. At this time, hydrophilic sulfonic acid groups are grafted onto sepiolite, which further improves the hydrophilicity of sepiolite. In this way, not only the toughening properties of fibers are retained but also the original compressive strength of cement paste is maintained. The modified sepiolite fiber can improve the toughness of cement slurry by forming uniformly dispersed cross-linked wire drawing distribution and a “tension-bridging” structure inside the slurry.

Data Availability

The data used to support the findings of this study are available from the corresponding author upon request.

Conflicts of Interest

The authors declare that they have no conflicts of interest.

Acknowledgments

This work was supported by the National Natural Science Foundation of China (Grant no. 51904034) and the National Science and Technology Major Project (Grant numbers 2016ZX05060 and 2017ZX05032004-004).

References

- [1] G. C. Howard and W. G. Bearden, “Casing packer,” U.S. Patent 3272517, 1966.
- [2] C. George and R. R. Gerke, “Dispersant and fluid loss additives for oil field cements,” U.S. Patent 4557763, 1985.
- [3] Q. Wang, Q. Zhu, T. Shao et al., “The rheological test and application research of glass fiber cement slurry based on plugging mechanism of dynamic water grouting,” *Construction and Building Materials*, vol. 189, pp. 119–130, 2018.
- [4] G.-F. Peng, W.-W. Yang, J. Zhao, Y.-F. Liu, S.-H. Bian, and L.-H. Zhao, “Explosive spalling and residual mechanical properties of fiber-toughened high-performance concrete subjected to high temperatures,” *Cement and Concrete Research*, vol. 36, no. 4, pp. 723–727, 2006.
- [5] V. C. Li and M. Maalej, “Toughening in cement based composites. Part II: fiber reinforced cementitious composites,” *Cement and Concrete Composites*, vol. 18, no. 4, pp. 239–249, 1996.
- [6] J. J. Guo, S. S. Zhang, Z. Z. Fan, Q. W. Liu, and J. G. Wang, “The application of fiber cement slurry used to prevent and block leak,” *Applied Mechanics and Materials*, vol. 423–426, pp. 1279–1282, 2013.
- [7] X. Fang, H. Yang, and Z. Gao, “Carbon fiber/titanium superhybrid composite,” in *Proceedings of the 2002 National Conference on Composite Materials*, Beijing, China, February 2002.
- [8] K. Zheng, D. Chen, C. Wang et al., “Study and application of basic property of new plastic additives in cement slurry with fiber,” *Natural Gas Industry*, vol. 25, no. 11, pp. 56–58, 2005.
- [9] S. F. Santos, J. d. A. Rodrigues, G. H. D. Tonoli et al., “Effect of colloidal silica on the mechanical properties of fiber-cement reinforced with cellulosic fibers,” *Journal of Materials Science*, vol. 49, no. 21, pp. 7497–7506, 2014.
- [10] V. D. Pizzol, L. M. Mendes, L. Frezzatti, H. Savastano Jr., and G. H. D. Tonoli, “Effect of accelerated carbonation on the microstructure and physical properties of hybrid fiber-cement composites,” *Minerals Engineering*, vol. 59, no. 3, pp. 101–106, 2014.
- [11] M. Li, Y. Yang, and X. Guo, “Carbon fiber reinforced mechanical properties of oil well cement,” *Acta Materialia Compositae Sinica*, vol. 32, no. 3, pp. 782–788, 2015.
- [12] M. Cao, C. L. Xu, and C. Zhang, “Rheology, fiber distribution and mechanical properties of calcium carbonate (CaCO₃) whisker reinforced cement mortar,” *Composites Part A: Applied Science and Manufacturing*, vol. 90, pp. 662–669, 2016.
- [13] Y. Wang, F. He, J. Wang, C. Wang, and Z. Xiong, “Effects of calcium bicarbonate on the properties of ordinary Portland cement paste,” *Construction and Building Materials*, vol. 225, pp. 591–600, 2019.
- [14] J. Wang, E. Liu, and L. Li, “Characterization on the recycling of waste seashells with Portland cement towards sustainable cementitious materials,” *Journal of Cleaner Production*, vol. 220, pp. 235–252, 2019.
- [15] Y. Wang, F. He, J. Wang, and Q. Hu, “Comparison of effects of sodium bicarbonate and sodium carbonate on the hydration and properties of Portland cement paste,” *Materials*, vol. 12, no. 7, p. 1033, 2019.
- [16] Y. Bu, R. Wang, and R. Cheng, “Performance of fiber cement slurry for well cementation,” *Oil Drilling & Production Technology*, vol. 27, no. 2, pp. 25–27, 2005.
- [17] Y. Bu, R. Wang, H. Mu et al., “Experimental study on anti channeling performance of fibrous cement,” *Natural Gas Industry*, vol. 28, no. 4, pp. 64–66, 2008.
- [18] L. Bokobza, A. Burr, G. Garnaud, M. Y. Perrin, and S. Pagnotta, “Fibre reinforcement of elastomers: nanocomposites based on sepiolite and poly(hydroxyethyl acrylate),” *Polymer International*, vol. 53, no. 8, 2004.
- [19] T. D. Hapuarachchi and T. Peijs, “Multiwalled carbon nanotubes and sepiolite nanoclays as flame retardants for polylactide and its natural fibre reinforced composites,” *Composites Part A: Applied Science and Manufacturing*, vol. 41, no. 8, pp. 954–963, 2010.
- [20] S. Balci, “Effect of heating and acid pre-treatment on pore size distribution of sepiolite,” *Clay Minerals*, vol. 34, no. 4, p. 647, 2010.
- [21] R. Jarabo, E. Fuente, A. Blanco, A. Moral, L. Izquierdo, and C. Negro, “Effect of sepiolite on the flocculation of suspensions of fibre-reinforced cement,” *Cement and Concrete Research*, vol. 40, no. 10, pp. 1524–1530, 2010.
- [22] H. Manuel, K. Núñez, G. Raúl, and J. C. Merino, “Sepiolite as replacement of short glass fibre in polyamide composites for injection moulding applications,” *Applied Clay Science*, vol. 162, pp. 129–137, 2018.
- [23] M. Suárez and E. García-Romero, “Variability of the surface properties of sepiolite,” *Applied Clay Science*, vol. 67–68, pp. 72–82, 2012.
- [24] E. Fuente, R. Jarabo, Á. Blanco, A. Moral, L. Izquierdo, and C. Negro, “Effect of sepiolite on retention and drainage of suspensions of fiber-reinforced cement,” *Construction and Building Materials*, vol. 24, no. 11, pp. 2117–2123, 2010.
- [25] C. Wu and S. Kou, “Effects of high-calcium sepiolite on the rheological behaviour and mechanical strength of cement pastes and mortars,” *Construction and Building Materials*, vol. 196, pp. 105–114, 2019.

- [26] Z. Zhi-Li, "On the construction craft of the concrete packing in cable pipes of cement slurry with fiber in the sepiolite," *Shanxi Architecture*, vol. 25, 2008, in Chinese.
- [27] X. ZhangS. Yang et al., "Acid activation treatment of sepiolite and its hydrophilic surface modification," *Non-Metallic Mines*, vol. 41, no. 1, pp. 49–52, 2018, in Chinese.
- [28] X. ZhangS. Yang et al., "Preparation and properties of poly (2,5-benzimidazole)/sulfonated sepiolite composite proton exchange membrane for application in low temperature fuel cells," *Polymeric Materials Science and Engineering*, vol. 34, no. 12, pp. 143–149, 2018.
- [29] S. Lazarević, I. Janković-Častvan, D. Jovanović, S. Milonjić, D. Janačković, and R. Petrović, "Adsorption of Pb^{2+} , Cd^{2+} and Sr^{2+} ions onto natural and acid-activated sepiolites," *Applied Clay Science*, vol. 37, no. 1, pp. 47–57, 2007.
- [30] S. Dikmen, G. Yilmaz, E. Yorukogullari, and E. Korkmaz, "Zeta potential study of natural- and acid-activated sepiolites in electrolyte solutions," *The Canadian Journal of Chemical Engineering*, vol. 90, no. 3, pp. 785–792, 2012.
- [31] L. Kai, "The mineralogy research of the sepiolite and its application in environment conservation," Master's thesis, Central South University, Changsha, China, 2008.



Hindawi

Submit your manuscripts at
www.hindawi.com

